Analyst

Cite this: *Analyst*, 2012, **137**, 939

www.rsc.org/analyst

PAPER

Synthesis of Ag nanoparticle-decorated 2,4,6-tris(2-pyridyl)-1,3,5-triazine nanobelts and their application for H_2O_2 and glucose detection†

Xiaoyun Qin,[a] Wenbo Lu,[a] Yonglan Luo,[a] Guohui Chang,[a] Abdullah M. Asiri,[bc] Abdulrahman O. Al-Youbi[bc] and Xuping Sun*[abc]

Received 21st October 2011, Accepted 28th November 2011
DOI: 10.1039/c2an15996a

The present paper reports on the first preparation of 2,4,6-tris(2-pyridyl)-1,3,5-triazine nanobelts (TPTNBs) by adjusting the pH value of the solution and the subsequent synthesis of Ag nanoparticle (AgNP)-decorated TPTNBs (AgNP-TPTNBs) by mixing an aqueous $AgNO_3$ solution with preformed TPTNBs without use of any external reducing agent. It is found that the resultant AgNP-TPTNBs exhibit notable catalytic performance for H_2O_2 reduction. A glucose biosensor was fabricated by immobilizing glucose oxidase (GOD) onto a AgNP-TPTNBs-modified glassy carbon electrode (GCE) for glucose detection. The constructed glucose sensor has a wide linear response range from 3 mM to 20 mM (r: 0.999) with a detection limit of 190 μM. It is further shown that this glucose biosensor can be used for glucose detection in human blood serum.

H_2O_2 sensors play an important role in the fields of chemistry, biology, clinical control, and environmental protection.[1] Up to now, many techniques including spectrometry, titrimetry, chemiluminescence, and electrochemistry have been employed for the determination of H_2O_2.[2] Among them, the electrochemical technique is a promising tool for the construction of simple, low-cost sensors owing to its high sensitivity, good selectivity and ease of operation.[2d] The intrinsic selectivity and sensitivity of enzymatic reactions have been used, where nanostructures are employed to immobilize the enzymes and reduce the possibility of protein denaturing.[3] It is also shown that Ag nanoparticles (AgNPs) exhibit good catalytic activity toward H_2O_2 reduction.[4] Song *et al.* have fabricated AgNPs on a type I collagen-modified electrode for H_2O_2 detection, but it required an electrodeposition process where some crucial variables need to be investigated.[5a] Zhao *et al.* have constructed a H_2O_2 sensor based on a multi-wall carbon nanotube (MWCNT)/AgNP nanohybrids modified gold electrode, but a MWCNT pretreatment process was required and AgNPs were produced under ultrasonic conditions.[5b] Lin *et al.* have demonstrated a AgNP/ZnO nanorod modified electrode could be used for H_2O_2 detection; however, a photoreduction process was involved to reduce Ag^+ on the ZnO nanorods.[5c] Recently, we have also constructed some electrochemical H_2O_2 sensors based on AgNPs because of their large specific surface area, good biocompatibility and conductivity.[6] On the other hand, glucose oxidase (GOD) can catalyze the oxidation of glucose to H_2O_2 and gluconolactone with saturated O_2. It makes it possible to detect glucose based on monitoring the production of H_2O_2.[7] Therefore, glucose detection can be achieved *via* the determination of H_2O_2 generated by GOD-catalyzed oxidation of glucose.[8] Furthermore, the advantages of simplicity, short response time, high sensitivity and excellent selectivity also develop the prospect of immobilization of GOD on the electrode surfaces.[9]

In the past decades, triazine has received great attention as a small molecular building block to construct an extended architecture through direction specific molecular interactions such as coordination bonds, hydrogen bonds, π–π stacking and C–H–π interactions.[10] In particular, the rigid multidentate polypyridyl ligands and different placement of the N-atom contained in the triazine show great diversity in coordination with a metal ion and exhibit ligand-directed self-assembly.[11]

In this paper, we report on the first preparation of 2,4,6-tris (2-pyridyl)-1,3,5-triazine nanobelts (TPTNBs) by adjusting the pH values of the solution and then the synthesis of AgNP-decorated TPTNBs (AgNP-TPTNBs) by mixing an aqueous $AgNO_3$ solution with preformed TPTNBs in the presence of sodium hydroxide whose role is to accelerate the reaction rate of the reduction of Ag(I) ions.[12] TPTNBs are used as the reductant and support in this synthesis. It is found that the resultant AgNP-TPTNBs exhibit notable catalytic performance for H_2O_2 reduction. Furthermore, we fabricate a glucose biosensor by immobilizing GOD on a AgNP-TPTNBs-modified glassy carbon electrode (GCE) for glucose detection because AgNPs can't

[a]*State Key Lab of Electroanalytical Chemistry, Changchun Institute of Applied Chemistry, Chinese Academy of Sciences, Changchun, 130022, Jilin, China. E-mail: sunxp@ciac.jl.cn. Fax: (+86) 431-85262065; Tel: (+86) 431-85262065*
[b]*Chemistry Department, Faculty of Science, King Abdulaziz University, Jeddah, 21589, Saudi Arabia*
[c]*Center of Excellence for Advanced Materials Research, King Abdulaziz University, Jeddah, 21589, Saudi Arabia*
† Electronic supplementary information (ESI) available: Experimental section and supplementary figures. See DOI: 10.1039/c2an15996a

catalyze the oxidation of glucose. The linear response range and detection limit is estimated to be from 3 mM to 20 mM (r: 0.999) and 190 μM, respectively.

Fig. 1A and 1B show the transmission electron microscopy (TEM) images of thus formed TPTNBs and AgNP-TPTNBs. It is observed that well-defined nanobelts about tens of micrometres in length and 50 to 100 nm in width are obtained, as shown in Fig. 1A. The formation of the nanobelt structure could be attributed to the effect of adjusting the pH value of the solution. Furthermore, it is found that the preformed TPTNBs can reduce Ag(I) ions into metallic Ag in our present study. Fig. 1B shows the TEM image of the TPTNBs after their incubation with an aqueous $AgNO_3$ solution in the presence of sodium hydroxide solution, indicating that many dark dots about tens of nanometres in size are observed on the surface of the TPTNBs. The chemical composition of the nanobelts and nanoparticle-decorated nanobelts is further determined by the energy-dispersed spectrum (EDS), as shown in Fig. 1C and 1D, respectively. The peaks of C and N are observed in Fig. 1C, indicating that the nanobelts are formed from 2,4,6-tris (2-pyridyl)-1,3,5-triazine. The Cl element is from the residual HCl solution. Compared with Fig. 1C, one additional intensive peak of Ag element is found in Fig. 1D, which will be assigned to the formed AgNPs. The Si and other peaks originate from the ITO substrate. All these observations indicate the formation of AgNP-TPTNBs and the formation mechanism is given as follows: TPTNBs can effectively adsorb Ag(I) ions *via* coordination of their pyridyl functional groups in the TPTNBs to Ag(I) ions and then reduce *in situ* the as-adsorbed Ag(I) ions to form AgNPs.[13] TPTNBs serve as the reductant and the support in this synthesis. Scanning electron microscopy (SEM) measurements have been used to estimate the roughness and surface morphology of the modified material, as shown in Fig. 2. The increasing roughness is observed in Fig. 2B comparing with that in Fig. 2A.

To testify the sensing application of the resultant AgNP-TPTNBs, we designed an enzymeless H_2O_2 sensor by direct deposition of the AgNP-TPTNBs on a bare GCE surface. The effect of the pH of the buffer solution on the sensor was

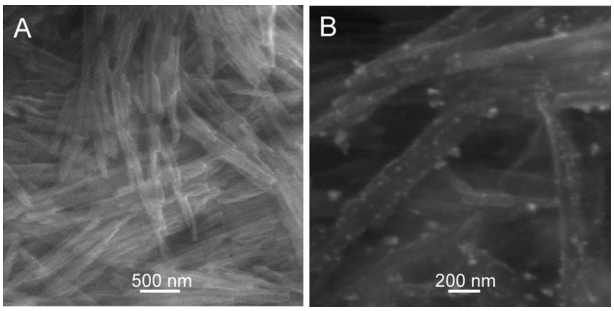

Fig. 2 Typical SEM images of TPTNBs (A) and AgNP-TPTNBs (B).

examined (Fig. S1†) and pH 6.5 was chosen for all experiments. Fig. 3 shows the cyclic voltammograms (CVs) of the bare GCE, TPTNB/GCE, citrate-protected AgNP-modified GCE (AgNP/GCE) and AgNP-TPTNB/GCE toward the reduction of H_2O_2 in 0.2 M PBS at pH 6.5. It is obviously seen that the responses of both the bare GCE and TPTNB/GCE toward the reduction of H_2O_2 are quite weak in the potential range between −0.2 and 0.8 V. In contrast, the AgNP-TPTNB/GCE exhibits a remarkable catalytic reduction current peak about 25 μA centered at −0.50 V *vs.* Ag/AgCl. Compared to the responses of AgNP/GCE, the AgNP-TPTNB/GCE toward the reduction of H_2O_2 exhibits a 0.10 V positive shift of the peak potential. It can be attributed to the changed mass transport and the existence of porosity in the AgNP-TPTNB/GCE surface due to the presence of TPTNBs.[14] It is also important to note that the AgNP-TPTNB/GCE exhibits no electrochemical response in the absence of H_2O_2. All the above observations indicate that the AgNPs contained in the nanocomposites exhibit notable catalytic performance for H_2O_2 reduction and the TPTNBs exhibit no catalytic activity. In addition, the relative standard deviation (RSD) of the amperometric response to 1 mM H_2O_2 was 3.9% for 10 successive measurements, indicating the good reproducibility of the AgNP-TPTNB/GCE. The stability of the sensor was tested by measuring the response currents of the electrode. After 30 days, only 10.4% signal of current was lost, indicating the good stability for H_2O_2 detection.

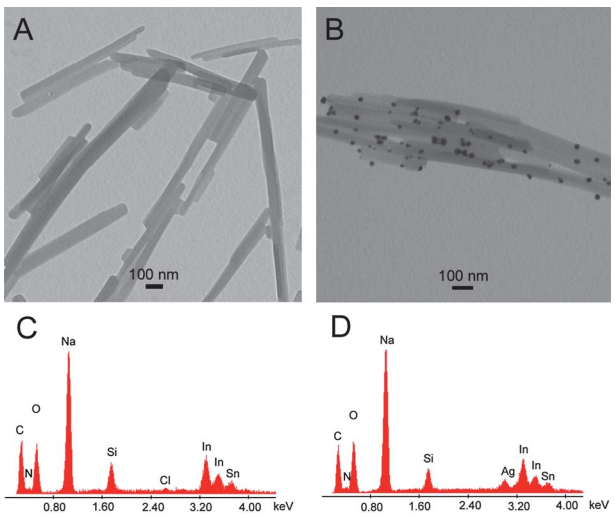

Fig. 1 Typical TEM images (A, B) and corresponding EDS (C, D) of TPTNBs and AgNP-TPTNBs.

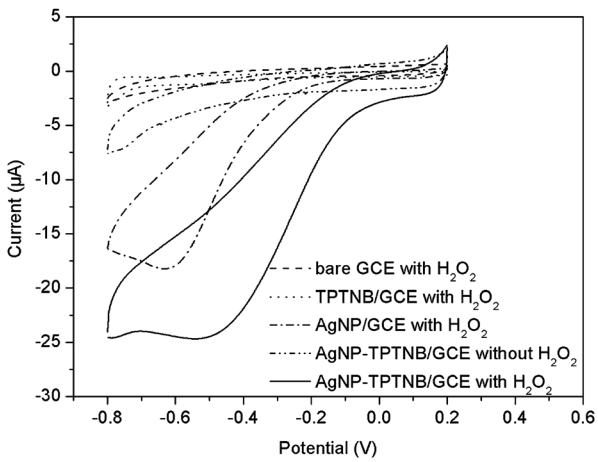

Fig. 3 CVs of different electrodes in N_2-saturated 0.2 M PBS at pH 6.5 in the presence and absence of 1 mM H_2O_2 (scan rate: 50 mV s^{-1}).

Fig. 4 shows a typical current–time plot of the AgNP-TPTNB/GCE in N_2-saturated 0.2 M PBS buffer (pH 6.5) on consecutive step change of H_2O_2 concentrations. Although the AgNP-TPTNB/GCE exhibits the biggest response signal at −0.50 V, determination of the H_2O_2 is carried out at −0.3 V. Such a low applied potential can ensure sufficient current response with lower background or less interference of other electroactive species in the solution.[5b] When an aliquot of H_2O_2 was dropped into the stirring PBS solution, the reduction current rose steeply to reach a stable value. The sensor could accomplish 95% of the steady state current within 2 s, indicating a fast amperometric response behavior. It is apparently seen that the steps shown in Fig. 4 are more horizontal in the region of lower concentration of H_2O_2 and the noises become higher with increased concentration of H_2O_2. Inset b (Fig. 4) shows the calibration curve of the sensor. The linear detection range is estimated to be from 0.1 mM to 60 mM (r: 0.985), and the detection limit is estimated to be 2.04 μM at a signal-to-noise ratio of 3. Although the detection limit is a little bit higher than some reported H_2O_2 biosensors,[15] the AgNP-TPTNB/GCE still exhibits improved detection limit, sensitivity, facility, and stability compared with other previous H_2O_2 biosensors.[16]

Fig. 5 shows CVs of the bare GCE, AgNP-TPTNB/GCE and GOD/AgNP-TPTNB/GCE in N_2-saturated PBS solution. It is found that no peak is observed for the bare GCE and AgNP-TPTNB/GCE. In contrast, the GOD/AgNP-TPTNB/GCE exhibits a clear electrochemical response. A pair of redox peaks at GOD/AgNP-TPTNB/GCE is observed. The formal potential ($E^{\circ\prime}$) calculated by averaging the cathodic and anodic peak potentials is estimated as ~0.44 V with ~110 mV peak-to-peak separation and ~1 ratio of cathodic to anodic current intensity. Compared to the CV curve of the AgNP-TPTNB/GCE, the well-defined redox peaks can be ascribed to GOD, which is characteristic of the reversible electron transfer process of the redox active center in the GOD.[17]

The adsorbed GOD still retains its specific enzyme activity, which is further verified by FT-IR measurements as shown in

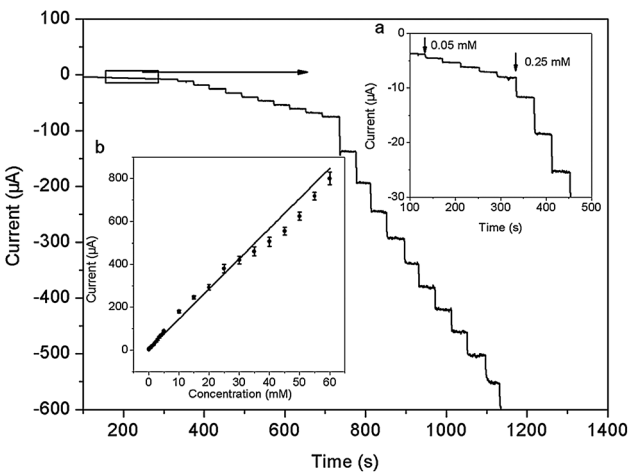

Fig. 4 Typical steady-state response of the AgNP-TPTNB/GCE to successive injection of H_2O_2 into the stirred N_2-saturated 0.2 M PBS at pH 6.5. Inset: (a) amplified response curve at low concentrations and (b) the corresponding calibration curve (Applied potential: −0.3 V).

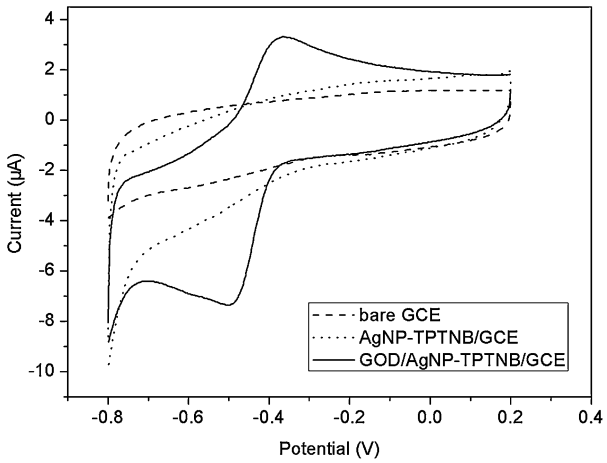

Fig. 5 CVs of bare GCE, AgNP-TPTNB/GCE and GOD/AgNP-TPTNB/GCE in 0.2 M PBS solution (pH: 7.4) saturated with N_2 at a scan rate of 300 mV s^{-1}.

Fig. S2†. The amide I and II infrared bands have been widely used for monitoring conformational changes in proteins.[18] The two amide bands, within ranges of 1700–1600 cm^{-1} and 1600–1500 cm^{-1}, are observed at both a GOD sample and AgNP-TPTNBs film covered with GOD. The former (1652 cm^{-1}, amide I band) is caused by C═O stretching vibrations of peptide linkages in the GOD backbone, whereas the latter (1525 cm^{-1}, amide II band) results from a combination of N–H in-plane bending and C–N stretching of the peptide groups. The AgNP-TPTNBs modified surface does not produce any spectral absorption in this wavelength range. The presence of these two distinctive absorption bands in Fig. S2† clearly suggests that the attachment of GOD onto AgNP-TPTNBs does not perturb the GOD conformations drastically. The small difference of the two spectra in Fig. S2† indicates that GOD retains its native conformation in the AgNP-TPTNBs film despite the small perturbation. Purposely denatured samples of GOD would show completely different spectral characteristics in the amide I and II regions.[19] All these observations indicate that the GOD still retains its bioactivity after adsorption on the AgNP-TPTNBs.

Due to its high binding specificity and turnover rate and relatively high stability, GOD has been the most frequently used glucose recognition element.[20] The following equations describe the oxidation of glucose in the presence of oxygen to form H_2O_2, which can be electrochemically detected.[7b,21] To testify the sensing application of the GOD/AgNP-TPTNB composites, we design a glucose biosensor by direct deposition of the AgNP-TPTNB, GOD and chitosan solution on a bare GCE surface successively.

$$\text{Glucose} + O_2 + H_2O \rightarrow \text{Gluconic acid} + H_2O_2 \quad (1)$$

$$H_2O_2 \rightarrow O_2 + 2H^+ + 2e^- \quad (2)$$

The biosensor toward the glucose oxidation of GOD/AgNP-TPTNB/GCE can be affected by a variety of parameters. Here, the effects of solution acidity and amount of GOD in preparing the biosensor were studied and the analytical conditions were optimized. The current response of the GOD/AgNP-TPTNB/

GCE to 4 mM glucose increased in the pH range of 6.0–7.4, and decreased at higher pH values (Fig. S3†). The decrease of current response in strong acidic and alkaline solutions might originate from the decrease in bioactivity of the enzyme.[22] The maximum current was obtained at pH 7.4, which was near the physiological condition and was chosen for subsequent experiments. The maximum current was obtained at 4 μL of 38 mg mL^{-1} of GOD loading (Fig. S4†).

Fig. 6 shows the electrocatalytic responses of the GOD/AgNP-TPTNB/GCE in 0.2 M PBS at pH 7.4 in the presence of various concentrations of glucose saturated with O_2. The signal responses of the GOD/AgNP-TPTNB/GCE on glucose with different concentrations were recorded in the solution of 0.2 M PBS (pH 7.4) *via* increasing the glucose concentration step by step. When the concentration of glucose increased from 3 mM to 20 mM, the amount of H_2O_2 generated by the GOD catalyzed oxidation of glucose increased quickly, and the current of the H_2O_2 reduction peaks at about −0.59 V presented a continuous increase, as shown in Fig. 6. The inset of Fig. 6 shows the catalytic current *versus* glucose concentration relationship. A good linear relationship is found between the catalytic current and glucose concentration range from 3 to 20 mM (*r*: 0.999). The detection limit of glucose is 190 μM. The RSD of the current response to 6 mM glucose is 4.1% for 5 successive measurements, indicating that the glucose biosensor has good reproducibility. Since the blood glucose levels of normal persons are in the range of 4 to 6 mM,[7a,23] our glucose biosensor may be used for glucose determination in real samples due to its wide linear response range.

When the glucose concentration was high, a plateau current was observed in the inset of Fig. 6, showing the characteristics of the Michaelis–Menten kinetic mechanism. The apparent Michaelis–Menten constant (K_m), which gives an indication of the enzyme-substrate kinetics, can be calculated from the Lineweaver–Burk equation:[24]

$$\frac{1}{I_{ss}} = \frac{1}{I_{max}} + \frac{I_m}{I_{max}} \times \frac{1}{C} \quad (3)$$

where I_{ss} is the steady-state current, I_{max} is the maximum current measured under saturated substrate conditions, and C is the concentration of the substrate. Using the slope and intercept from the Lineweaver–Burk plot (Fig. S5†), we estimated the value of K_m for the GOD/AgNP-TPTNB/GCE as 25.1 mM. The value is close to the reported value for the free enzyme,[25] illustrating the non-denaturating character of the enzyme anchoring procedure. In order to assess the analytical performance level of the proposed biosensor, the characteristics of the proposed biosensor were compared with other glucose biosensors as shown in Table S1†. The results have shown that the linearity range, detection limit and sensitivity of the proposed biosensor are better than the previously reported models.[7a,8,9b,26]

The detection at positive potential (0.7 V) may be interfered by some related biomolecules such as ascorbic acid (AA), dopamine (DA), acetaminophen (AP) and uric acid (UA) by oxidation in practical clinical analysis.[27] So the reduction detection by the modified biosensor is more suitable.[17] This conclusion has been confirmed by an amperometric method as shown in Fig. S6†. The current responses of the interferents were negligible compared to that induced by the glucose, indicating the present glucose biosensor was feasible for the determination of glucose in the presence of common interfering compounds. In this regard, it is maybe worth reminding that a low concentration of interferences is used because the average concentration of AA in blood is 0.05–0.143 mM,[28a] the average concentration of AP is 0.066–0.2 mM,[28b] and the average concentration of UA is 0.5 mM,[28c] and much smaller than that of glucose (normal range: 4–6 mM), it also has a negligible effect on the glucose detection in serum samples.

To testify the feasibility of the GOD/AgNP-TPTNB/GCE in practical analysis, we employed the biosensor to measure glucose in human blood serum. The original glucose concentrations of the human serum samples were first evaluated accurately by Institute of Virology and AIDS Research, First Affiliated Hospital, Jilin University, Changchun, Jilin, People's Republic of China. The samples were then reassayed with the GOD/AgNP-TPTNB/GCE. Fig. 7 shows a calibration curve of glucose concentration in human blood serum using the standard addition method for GOD/AgNP-TPTNB/GCE. The initial amperometric response in human blood serum after stabilization of the background is 23 ± 1 μA, which is very close to the response of 6 mM glucose. It can be seen that the sensor is linear up to

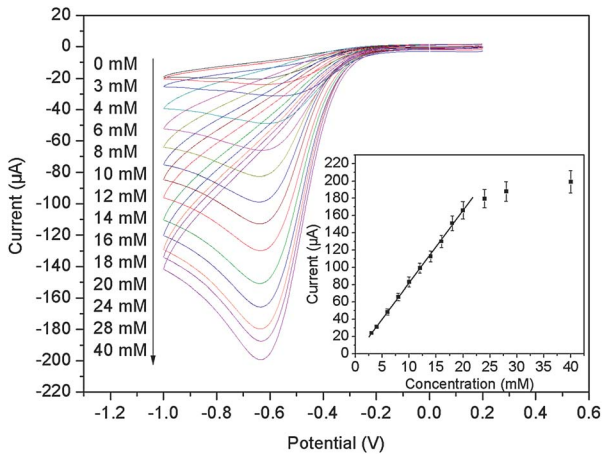

Fig. 6 CVs of the GOD/AgNP-TPTNB/GCE in PBS solution (pH 7.4) in the presence of various concentrations of glucose saturated with O_2. Inset is the calibration curve (*r*: 0.999) corresponding to amperometric responses at the reduction peak.

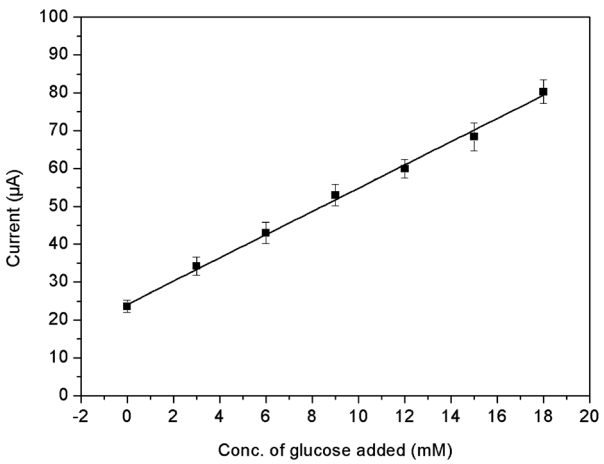

Fig. 7 Calibration plot of glucose concentration in human blood serum by use of the standard addition method.

Table 1 Results of glucose determination in human blood serum

Sample	Determined by our sensor (mM)	Measured by local hospital (mM)	RSD (%)
1	6.05	5.55	4.3
2	6.77	6.36	3.9
3	7.65	7.49	2.9

18 mM glucose. The contents of glucose in serum can then be calculated from the calibration curve. As shown in Table 1, the results are satisfactory and agree closely with those measured in the hospital.

The long-term stability of the prepared glucose biosensor is a critical factor in practical application. To evaluate the stability of the glucose biosensor, the GOD/AgNP-TPTNB/GCE was stored at 4 °C when not in use. The stability was examined by periodical measurements of the biosensor responses to 3 mM glucose in PBS solution (pH 7.4) at a scan rate of 50 mV s^{-1}. The variation of the response current at the GOD/AgNP-TPTNB/GCE decreased to about 93% of its initial response current on the 2nd day and about 73% after 40 days, as shown in Fig. S7†. The loss of the response current may be ascribed to the decrease of the enzyme activity during these days.[8]

In summary, we have demonstrated successfully the preparation of TPTNBs and AgNP-TPTNBs for the first time. It suggests such AgNP-TPTNBs show notable catalytic performance toward the reduction of H_2O_2. The use of such AgNP-TPTNBs as building blocks for the construction of a biosensor for glucose detection in both buffer and human blood serum has also been demonstrated successfully. Overall, the high sensitivity, good selectivity, large linear range and long time stability exhibited by the biosensor make it a good candidate for glucose measurements in biological samples and for real time glucose monitoring.

Acknowledgements

This work was supported by the National Natural Science Foundation of China (No. 21175129) and the National Basic Research Program of China (No. 2011CB935800).

Notes and references

1 (*a*) X. Shu, Y. Chen, H. Yuan, S. Gao and D. Xiao, *Anal. Chem.*, 2007, **79**, 3695; (*b*) B. Wang, J. Zhang, Z. Pan, X. Tao and H. Wang, *Biosens. Bioelectron.*, 2009, **24**, 1141.
2 (*a*) Y. Song, L. Wang, C. Ren, G. Zhu and Z. Li, *Sens. Actuators, B*, 2006, **114**, 1001; (*b*) P. A. Tanner and A. Y. S. Wong, *Anal. Chim. Acta*, 1998, **370**, 279; (*c*) R. Dringen, L. Kussmaul and B. Hampreeht, *Brain Res. Protoc.*, 1998, **2**, 223; (*d*) M. N. Bui, X. Pham, K. N. Han, C. A. Li, Y. S. Kim and G. H. Seong, *Sens. Actuators, B*, 2010, **150**, 436.
3 (*a*) I. Willner and E. Katz, *Angew. Chem., Int. Ed.*, 2000, **39**, 1180; (*b*) Y. Xiao, F. Patolsky, E. Katz, J. Hainfeld and I. Willner, *Science*, 2003, **299**, 1877.
4 A. Liu, W. Dong, E. Liu, W. Tang, J. Zhu and J. Han, *Electrochim. Acta*, 2010, **55**, 1971.
5 (*a*) Y. Song, K. Cui, L. Wang and S. Chen, *Nanotechnology*, 2009, **20**, 105501; (*b*) W. Zhao, H. Wang, X. Qin, X. Wang, Z. Zhao, Z. Miao, L. Chen, M. Shan, Y. Fang and Q. Chen, *Talanta*, 2009, **80**, 1029; (*c*) C. Lin, Y. Lai, A. Balamurugan, R. Vittal, C. Lin and K. C. Ho, *Talanta*, 2010, **82**, 340.
6 (*a*) S. Liu, J. Tian, L. Wang, H. Li, Y. Zhang and X. Sun, *Macromolecules*, 2010, **43**, 10078; (*b*) J. Tian, S. Liu and X. Sun, *Langmuir*, 2010, **26**, 15112; (*c*) W. Lu, F. Liao, Y. Luo, G. Chang and X. Sun, *Electrochim. Acta*, 2011, **56**, 2295; (*d*) J. Tian, H. Li, W. Lu, Y. Luo, L. Wang and X. Sun, *Analyst*, 2011, **136**, 1806; (*e*) X. Qin, W. Lu, Y. Luo, G. Chang and X. Sun, *Electrochem. Commun.*, 2011, **13**, 785.
7 (*a*) C. Shan, H. Yang, D. Han, Q. Zhang, A. Ivaska and L. Niu, *Biosens. Bioelectron.*, 2010, **25**, 1070; (*b*) W. Jia, K. Wang and X. Xia, *TrAC, Trends Anal. Chem.*, 2010, **29**, 306.
8 (*a*) W. Lu, Y. Luo, G. Chang and X. Sun, *Biosens. Bioelectron.*, 2011, **26**, 4791; (*b*) Y. Zhang, G. Chang, S. Liu, W. Lu, J. Tian and X. Sun, *Biosens. Bioelectron.*, 2011, **28**, 344.
9 (*a*) Y. Sun, Y. Bai, W. Yang and C. Sun, *Electrochim. Acta*, 2007, **52**, 7352; (*b*) M. Ammam and E. B. Easton, *Sens. Actuators, B*, 2011, **155**, 340.
10 (*a*) G. R. Desiraju, *Acc. Chem. Res.*, 1996, **29**, 441; (*b*) A. Das, C. Marschner, J. Cano, J. Baumgartner, J. Ribas, M. S. E. Fallah and S. Mitra, *Polyhedron*, 2009, **28**, 2436.
11 (*a*) L. N. Dawe, K. V. Shuvaev and L. K. Thompson, *Chem. Soc. Rev.*, 2009, **38**, 2334; (*b*) M.-L. Cao, J.-J. Wu, J.-J. Liang and B.-H. Ye, *Cryst. Growth Des.*, 2010, **10**, 4934.
12 K. S. Chou and Y. S. Lai, *Mater. Chem. Phys.*, 2004, **83**, 82.
13 (*a*) L. Zhang, X. Q. Lü, Q. Zhang, C. L. Chen and B. S. Kang, *Transition Met. Chem.*, 2005, **30**, 76; (*b*) S. Thanjam, M. F. Philips, S. Komathi, P. Manisankar, C. Sivakumar, A. Gopalan and K. P. Lee, *Spectrochim. Acta, Part A*, 2011, **79**, 1256.
14 (*a*) F. W. Campbell, S. R. Belding, R. Raron, L. Xiao and R. G. Compton, *J. Phys. Chem. C*, 2009, **113**, 9053; (*b*) X. Dai, G. G. Wildgoose, C. Salter, A. Crossley and R. G. Compton, *Anal. Chem.*, 2006, **78**, 6102.
15 (*a*) Z. Cao, X. Jiang, Q. Xie and S. Yao, *Biosens. Bioelectron.*, 2008, **24**, 222; (*b*) C. Chen, C. Sun and Y. Gao, *Electrochem. Commun.*, 2009, **11**, 450.
16 (*a*) C. Guo, Y. Song, H. Wei, P. Li, L. Wang, L. Sun, Y. Sun and Z. Li, *Anal. Bioanal. Chem.*, 2007, **389**, 527; (*b*) J. Tian, H. Li, W. Lu, Y. Luo, L. Wang and X. Sun, *Analyst*, 2011, **136**, 1806.
17 C. Shan, H. Yang, J. Song, D. Han, A. Ivaska and L. Niu, *Anal. Chem.*, 2009, **81**, 2387.
18 (*a*) T. F. Kumosinski and J. J. Unruh, *Molecular Modeling. ACS Symp. Ser.*, 576, Washington DC, 1993, pp71–98; (*b*) X. H. Chen, H. Xie, J. L. Kong and J. Q. Deng, *Biosens. Bioelectron.*, 2001, **16**, 115.
19 L. Wang and Z. Yuan, *Sensors*, 2003, **3**, 544.
20 K. E. Toghill and R. G. Compton, *Int. J. Electrochem. Sci.*, 2010, **5**, 1246.
21 M. Tsai and Y. Tsai, *Sens. Actuators, B*, 2009, **141**, 592.
22 Q. Zeng, J.-S. Cheng, X.-F. Liu, H.-T. Bai and J.-H. Jiang, *Biosens. Bioelectron.*, 2011, **26**, 3456.
23 M. Ammam and J. Fransaer, *Sens. Actuators, B*, 2010, **145**, 46.
24 R. A. Kamin and G. S. Wilson, *Anal. Chem.*, 1980, **52**, 1198.
25 B. E. P. Swoboda and V. Massey, *J. Biol. Chem.*, 1965, **240**, 2209.
26 (*a*) X. Chou, D. Duan, G. Shen and R. Yu, *Talanta*, 2007, **71**, 2040; (*b*) Y. M. Unag and T. C. Chou, *Biosens. Bioelectron.*, 2003, **19**, 141; (*c*) G. Fu, X. Yue and Z. Dai, *Biosens. Bioelectron.*, 2011, **26**, 3973; (*d*) X. Kang, J. Wang, H. Wu, I. A. Aksay, J. Liu and Y. Lin, *Biosens. Bioelectron.*, 2009, **25**, 901.
27 Z. H. Wang, J. Liu, Q. L. Liang, Y. M. Wang and G. Luo, *Analyst*, 2002, **127**, 653.
28 (*a*) J. P. Moran, L. Cohen, J. M. Greene, G. Xu, E. B. Feldman, C. G. Hames and D. S. Feldman, *Am. J. Clin. Nutr.*, 1993, **57**, 213; (*b*) A. Kratz, M. Ferraro, P. M. Sluss and K. B. Lewandrowskic, *N. Engl. J. Med.*, 2004, **351**, 1548; (*c*) M. Grootveld and B. Hallowell, *Biochem. J.*, 1987, **243**, 803.